Radiation and Environmental Biophysics (2022) 61:407–423
https://doi.org/10.1007/s00411-022-00983-5

ORIGINAL ARTICLE

Association between the cardiac contact distance and the maximum dose at the left anterior descending coronary artery in post mastectomized patients

A. H. Badillo-Alvarado[1] · E. A. Martín-Tovar[1] · G. M. Molina-Salinas[2] · A. C. Sandoval-Méndez[1] · A. Sarricolea-Puch[1]

Received: 20 May 2021 / Accepted: 26 June 2022 / Published online: 11 July 2022

Abstract

The clinical information on the relationship between the cardiac contact distance (CCD), the maximum dose (D_{max}) delivered to the left anterior descending (LAD) coronary artery and the mean heart dose has mostly focused on patients with breast-conserving surgery (BCS), being scarce in postmastectomy patients. The aim of this study is to determine the association between the CCD and the D_{max} delivered to the LAD. The secondary objective was to evaluate the dosimetric results of comparing three-dimensional conformal radiotherapy (3D-CRT) to intensity-modulated radiotherapy (IMRT) and volumetric modulated arc therapy (VMAT) techniques for post mastectomized breast cancer patients with irradiation to the left chest wall. 53 cases of women who received adjuvant standard fractionated postmastectomy radiotherapy (PMRT) were used. Three types of plans were created for each patient: 3D-CRT, seven equidistant IMRT fields, and four partial VMAT arcs. Correlations were evaluated using Pearson's correlation coefficient. Plans made with IMRT and VMAT showed improved homogeneity and conformity. Associations between CCD and D_{max} to LAD were positive for all three plan types. Compared to 3D-CRT, the modulated intensity plans obtained better dose homogeneity and conformity to the target volume. The LAD and heart doses were significantly lower for IMRT and VMAT plans. The CCD can be used as a predictor of the maximum and mean doses of the LAD. Modulated intensity techniques allow for better dose distribution and dose reduction to the heart and LAD.

Keywords Breast cancer · Radiotherapy · Left anterior descending coronary artery · Cardiac contact distance · Postmastectomy

Introduction

Breast-conserving surgery (BCS) and mastectomy followed by adjuvant radiotherapy are the standard treatments for breast cancer. Since many patients have a favorable prognosis, it is necessary to study the possible toxicities associated with radiotherapy treatment for their post-treatment quality of life.

The heart is one of the most radiosensitive organs in the human body since it is susceptible to both early and late toxicities. This is particularly important in women with left breast cancer, due to its proximity to the treatment region. A population-based study found that the risk of cardiac death is 1.7 times higher in patients who received adjuvant whole breast radiation therapy (WBRT) compared to those who were treated with surgery alone (Darby et al. 2005, 2013). The risk was considerably higher in patients with left-sided cancer. It was also pointed out that there is a linear relationship between the mean heart dose (MHD) and an increased risk of major cardiac events, this strengthens the relationship between radiotherapy and cardiac damage (Darby et al. 2013). Increasing the MHD by 1 Gy produces a 7.4% increase in the risk of major coronary events (Darby et al. 2013). Another study states that adding 1 Gy of irradiation

✉ E. A. Martín-Tovar
enrique.martin.tovar@gmail.com

[1] División de Oncología y Uronefrología, Departamento de Radioterapia, Unidad Médica de Alta Especialidad, Hospital de Especialidades del Centro Médico Nacional "Ignacio García Téllez", Instituto Mexicano del Seguro Social, CP 97150 Mérida, Yucatán, México

[2] Unidad de Investigación Médica Yucatán, Unidad Médica de Alta Especialidad Hospital de Especialidades 1 Mérida, Yucatán, Instituto Mexicano del Seguro Social, CP 97150 Mérida, Yucatán, México

to the MHD increases the risk of cardiotoxicity by 4% (Mège et al. 2011).

For radiotherapy (RT) treatments, in general, the entire heart is considered a single organ at risk (OAR). Nevertheless, recent studies consider that the dose to the coronary arteries could be a better predictor of radiation-induced toxicity in comparison to the whole heart dose (Borger et al. 2007; Bramkamp et al. 2007; Hector and Trott 2007; Gagliardi et al. 2010; Aznar et al. 2011; Poortmans et al. 2012); particularly to the left anterior descending (LAD) coronary artery, which is one of the most frequent sites of RT-related ischemic heart disease (Hector and Trott 2007). The LAD is more sensitive to radiation compared to myocardial tissue (Tan et al. 2012), so it is suggested that the dose delivered to the heart is not entirely reliable in determining the LAD dose (Tan et al. 2012); consequently it should be considered as an independent OAR. Nonetheless, it is not customary to contour the LAD for RT, this is partly due to the difficulty in delineating its narrow volume, as well as that it may not be necessary to specifically contour the coronary arteries as long as the Radiation Therapy Oncology Group (RTOG) guidelines are met (Shekel et al. 2014).

Meanwhile, numerous studies have sought to make use of anatomical characteristics as instruments to predict the radiation dose to the heart during RT. Lee et al. (2015) evaluated 80 women whose cohort characteristics were a diagnosis of left breast cancer treated with adjuvant RT without respiratory control, and found a correlation between the MHD and what they called cardiac contact distance (CCD), defining it as the length (measured in mm) in the parasagittal plane where any part of the thoracic wall makes contact with any part of the heart. There is a study that shows a correlation between the maximum dose (D_{max}) delivered to the LAD and the CCD (Mendez et al. 2018). However, both studies focus on patients undergoing BCS. Information remains scarce for women undergoing mastectomy. Therefore, the aim of the present work is to study the possible association between the CCD and the D_{max} delivered to the LAD for postmastectomy radiotherapy (PMRT) patients. The secondary objective was to compare the dosimetric results obtained from the three-dimensional conformal radiation therapy (3D-CRT) with intensity-modulated radiation therapy (IMRT) and volumetric modulated arc therapy (VMAT) techniques.

Materials and methods

Patient selection and planning

A retrospective review of the treatment records of 53 patients was conducted to quantitatively assess a cohort of women with histologically confirmed invasive left-sided breast cancer that underwent PMRT carried out at the authors' clinic from January to December 2019. Patients who met the following criteria were excluded: women with a diagnosis of right breast cancer, previous RT to the chest, a diagnosis of bilateral breast cancer who had received RT to both chest walls, men with breast cancer, and diagnosis of the synchronous primary tumor.

The computed tomography (CT) simulation was performed with a single-energy 64-slice Siemens SOMATOM Definition AS VA44A scanner (Siemens Healthineer, Germany). All CT scans were acquired during free breathing (FB). The patient was set up in a supine position with both arms raised and abducted at approximately 90°–120°. The patient's head was turned to the right. The axial slice thickness was 5 mm, in agreement with the institutional protocol of the authors' workplace. The CT scans were not contrast enhanced and were acquired from the C1 to L1 vertebrae. Subsequently, all digital imaging and communications in medicine (DICOM) 3D-CT image data sets were transferred to the Eclipse Treatment Planning System (TPS) (v. 16.1, Varian Medical Systems; Palo Alto, CA, USA).

All patients had a standard fractionated PMRT (50 Gy in 25 fractions or 50.4 Gy in 28 fractions) over five to six weeks. The left chest wall or left chest wall with lymph nodes (axillary levels I, II, III, and supraclavicular) were considered in the clinical judgment of the radiation oncologist as the clinical target volume (CTV) according to the RTOG breast cancer contouring guidelines (White et al. 2018). The planning target volume (PTV) was generated by expanding isotropically 7 mm from the CTV and it was trimmed 3 mm from the skin's surface. According to the authors' institutional local practice, the internal mammary nodes (IMN) were not included in the CTV. The contoured OARs were: heart, which starts just inferior to the left pulmonary artery and ends in the diaphragm, it should encompass the pericardium to include the cardiac vessels, in accordance to the Feng atlas (Feng et al. 2011); the LAD coronary artery, which was delimited from the end of the left main coronary artery behind the pulmonary artery extending to the apex of heart, running in the interventricular groove, according to the proposal by Duane et al. (2017). Additionally, the LAD-PRV (planning organ at risk volume) auxiliary structure was generated around the LAD by adding an anisotropic margin (Fig. 1a, b.) with a diameter of 6 mm in the anterior–posterior direction and 10 mm from left to right, similar to what was proposed by Duma (2017). By using the TPS length measurement tool, the CCD was measured in a free-breathing CT on the parasagittal plane, as indicated by Lee et al. (2015) (Fig. 2). All contouring was done by the same radiation oncologist. The heart constraints were in accordance to QUANTEC (Gagliardi et al. 2010).

The same medical physicist generated three different plans for each patient, namely, 3D-CRT, IMRT and VMAT plans. All plans were made on the same set of CT images

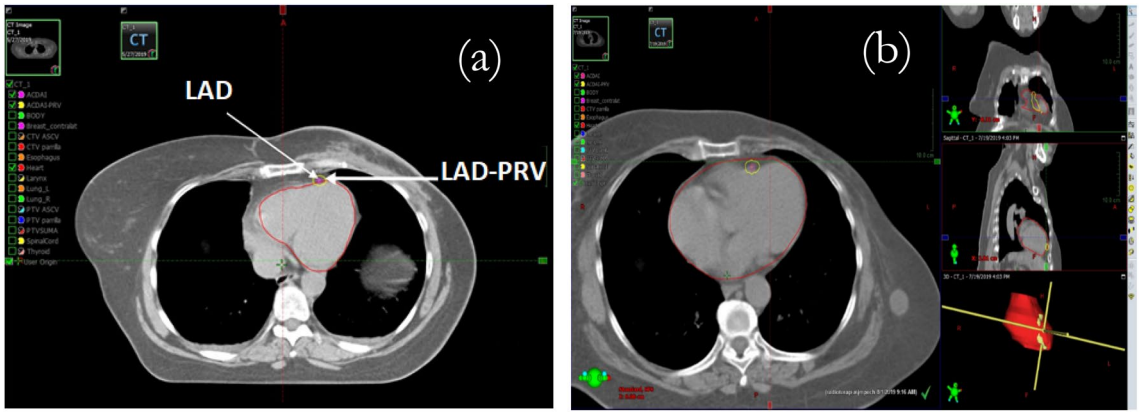

Fig. 1 CT of **a** axial view of the LAD in pink (thin line) and of the LAD-PRV in yellow **b** view of the LAD and LAD-PRV the three visualization planes

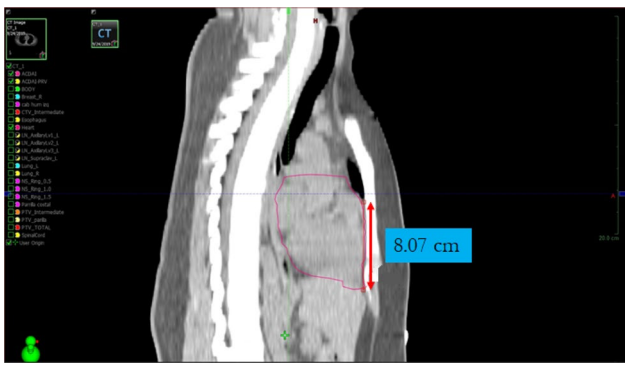

Fig. 2 Cardiac contact distance measurement in the parasagittal plane (red arrow)

and reviewed by a senior radiation oncologist. At least 95% of the prescription dose was intended to be delivered to 95% of the PTV volume. To make a fair comparison between the three techniques, all plans were normalized to this dose-volume point value. The AAA algorithm (anisotropic analytical algorithm) was used in a Varian VitalBeam Linac equipped with a 120-leaf MLC using 6 MV beams, with a grid size of 2.5 mm.

All patients were originally treated using the 3D-CRT technique using two opposing tangential coplanar fields. The orientation of the beams was chosen to avoid angles directed toward critical normal structures (Rudat et al. 2011; Duma 2017). Gantry angles ranged from 300° to 310° for the anterior field, and from 120° to 130° for the posterior field. An angle of 0° was chosen for both the collimator and couch. Wedges were not used. The dose delivered to the LAD was not taken into account in the planning process (Mendez et al. 2018). The 3D-CRT plans were the treatments originally delivered to the 53 patients in 2019. LAD contouring at that time was not standard at the authors' workplace and was therefore not considered as an OAR. Subsequently, all cases were replanned using IMRT and VMAT to analyze the dosimetric differences between the three techniques in terms of doses delivered to the LAD and to the heart. In both modulated intensity modalities, the dose given to the LAD was restricted during the planning process (this was not possible with the two tangential fields of the 3D-CRT plans). IMRT plans were created with seven equally spaced coplanar fields. They were placed in an angular sector of 230° in an axial plane around the left side of the patients. Gantry angles ranged from 300° to 170° (Popescu et al. 2006; Fogliata et al. 2007). Angles of 0° were established for both the collimator and couch. The sliding window technique was used with a fixed-dose rate of 600 Monitor-units/minute. Adequate dose coverage to the PTV was established as the highest priority in the optimization algorithm followed by the dose received from the OARs. In particular, it was sought to reduce the doses to the LAD and LAD-PRV as much as possible without compromising the dose delivered to the PTV. VMAT plans were generated with the same voltage as IMRT and 3D-CRT plans, but with a maximum dose rate of 600 monitor-units/minute. The plans consisted of four coplanar fields of partial arcs with an angular extension of 230°. Two arcs rotated clockwise from 300° to 170°. The remaining two arcs rotated counterclockwise from 170° to 300° (Virén et al. 2015; Kang et al. 2019). Collimator angles of 30° and 330° were used for the clockwise and counterclockwise arcs, respectively. These collimator angles were chosen to limit the Tongue and Groove effect (Huang et al. 2014). The field size was restricted to 15 cm since this is recommended to allow both sides of the MLC to reach all sides of the field and thus improve dose coverage to the PTV (Ugurlu and Temelli 2020). A couch angle of 0° was selected for all arcs.

Dosimetric evaluation

A dose-volume histogram (DVH) was generated to perform a quantitative analysis of the PTV and OARs. The conformity index (*CI*) was calculated using Eq. 1 (Lin et al. 2015):

$$\mathrm{CI} = \frac{V_{\mathrm{PTV,ref}}}{V_{\mathrm{PTV}}} \times \frac{V_{\mathrm{PTV,ref}}}{V_{\mathrm{ref}}}, \quad (1)$$

where $V_{\mathrm{PTV,ref}}$ refers to the volume of the 95% of the prescribed dose that covers the PTV, V_{PTV} refers to the volume of the PTV, and V_{ref} is the volume of the 95% prescribing dose curve. The CI value is between 0 and 1, a CI value close to 1 indicates an ideal dose conformity. The homogeneity index (HI) was calculated with Eq. 2 (Ramasubramanian et al. 2019):

$$\mathrm{HI} = \frac{D_{2\%} - D_{98\%}}{D_{50\%}}, \quad (2)$$

where $D_{2\%}$, $D_{98\%}$ and $D_{50\%}$ represent the doses received by 2% (near maximum dose), 98% (near-minimum dose), and 50% of PTV's volume, respectively. A dose distribution with high homogeneity would have an HI of 0. Maximum (D_{max}) and mean (D_{mean}) doses for LAD and LAD-PRV were evaluated. Regarding the heart, MHD and $V_{25\mathrm{Gy}}$ (the percentage of heart volume that received a dose of 25 Gy) were recorded.

Statistical analysis

All data were subjected to the Kolmogorov–Smirnov normality test. To analyze the dosimetric differences between the three planning techniques, the paired, two tails Student's *t*-test was applied, and for non-normally distributed data the Wilcoxon signed ranks test was performed. The association between variables (CCD and D_{max} to the LAD, among others) was determined by calculating Pearson's correlation coefficient. The threshold for statistical significance was $p < 0.05$. The statistical analyses were performed using the OriginPro Software Version 2018 (OriginLab Corporation, Northampton, MA, USA).

A sensitivity power analysis (Faul et al. 2007) was performed to determine to what extent the Pearson coefficient would be reliable enough to detect effect sizes according to Cohen's guidelines (Cohen 1988, 1992) (Since the correlation coefficient *r* is the measure of the effect size). These guidelines classify effect sizes as small, medium, and large for Pearson's *r* values of 0.10, 0.30, and 0.50, respectively (Cohen 1988, 1992). This was also done to estimate sample size limitations. Power analysis was performed using the statistical analysis software G*Power (Version 3.1.9.7, Heinrich-Heine-Universität, Düsseldorf, Germany) (Faul et al. 2009) with a sample size of 53 patients, a significance level (α) of 0.05 and a statistical power ($1 - \beta$) of 0.80 (Chaikh et al. 2014).

Results

The average age was found to be 55.62 ± 13.69 years (range 31–89 years). The most frequent clinical stages were IIB and IIIA, which together corresponded to 32 cases (accounting for 60.36% of the sample). The mean PTV volume was 660.63 ± 233.45 cm^3 (range 268–1393.10 cm^3). Clinically acceptable dose distributions were obtained for all plans. The CCD had an average length of 43.72 ± 17.13 mm (range 0–87 mm).

Table 1 shows the dosimetric parameters of the PTV and OARs for the three techniques. Each parameter shows its standard deviation (SD). The *p*-values where a statistical difference is observed are marked in bold. The quality indices (CI and HI) revealed that the plans made with the IMRT and VMAT techniques have better homogeneity and conformity compared to the 3D-CRT plans. The CI and HI values for the 3D-CRT plans were 0.5156 ± 0.1462 and 0.1812 ± 0.0728, respectively. For the IMRT plan, they were 0.8587 ± 0.0477 and 0.1164 ± 0.0211, respectively. And for the plans made with VMAT they were 0.8615 ± 0.0448 and 0.1128 ± 0.0263, respectively. For *CI*, significant differences were found when comparing the 3D-CRT plans with IMRT ($p < 0.001$) and VMAT ($p < 0.001$) plans. A significant difference in *HI* was also observed when comparing 3D-CRT with IMRT ($p = 0.019$) and VMAT ($p = 0.016$). There was no significant difference between the IMRT and VMAT plans in terms of *CI* ($p = 0.787$) and HI ($p = 0.478$).

Doses to the LAD were substantially reduced using modulated intensity techniques. The D_{max} to the LAD was 45.96 ± 6.70 Gy (range 12.16—57.10 Gy) for 3D-CRT, 22.51 ± 5.08 (range 12.88–34.43 Gy) for IMRT and 22.95 ± 7.11 (range 12.40–45.04 Gy) for VMAT. For the D_{max} delivered to the LAD, significant differences were observed when comparing 3D-CRT with IMRT ($p < 0.001$) and VMAT ($p < 0.001$). A reduction in D_{max} of 51.02% and 50.06% was observed for IMRT and VMAT, respectively. The D_{mean} to the LAD was 34.68 ± 10.13 Gy (range 3.55—51.55 Gy) for 3D-CRT, 16.20 ± 4.21 (range 8.13- 27.26 Gy) for IMRT and 16.50 ± 5.61 (range 7.83–35.85 Gy) for VMAT. There were significant differences between 3D-CRT compared to IMRT ($p < 0.001$) and VMAT ($p < 0.001$). The D_{mean} reduction was 53.29% and 52.42% for IMRT and VMAT plans, respectively. No significant differences were observed in either D_{max} or D_{mean} delivered to the LAD when comparing IMRT to VMAT.

Modulated intensity techniques also produced a significant reduction in the D_{max} and D_{mean} delivered to LAD-PRV. The D_{max} to the LAD-PRV was 48.82 ± 4.77 Gy

Table 1 PTV dosimetric parameters for the 3D-CRT, IMRT and VMAT plans

Structure	Parameter	3D-CRT (mean ± SD)	IMRT (mean ± SD)	VMAT (mean ± SD)	*p*-value		
					3DCRT vs IMRT	3DCRT vs VMAT	IMRT vs VMAT
PTV	CI	0.5156 ± 0.1462 (0.2559–0.7800)	0.8587 ± 0.0477 (0.7968–0.9761)	0.8615 ± 0.0448 (0.7942–0.9660)	**< 0.001**	**< 0.001**	0.787
	HI	0.1812 ± 0.0728 (0.1043–0.3181)	0.1164 ± 0.0211 (0.0978–0.1722)	0.1128 ± 0.0263 (0.0769–0.1718)	**0.019**	**0.016**	0.478
LAD	D_{max} (Gy)	45.96 ± 6.70 (12.16—57.10)	22.51 ± 5.08 (12.88–34.43)	22.95 ± 7.11 (12.40–45.04)	**< 0.001**	**< 0.001**	0.256
	D_{mean} (Gy)	34.68 ± 10.13 (3.55—51.55)	16.20 ± 4.21 (8.13–27.26)	16.50 ± 5.61 (7.83–35.85)	**< 0.001**	**< 0.001**	0.318
LAD-PRV	D_{max} (Gy)	48.82 ± 4.77 (24.40–54.94)	37.70 ± 7.43 (19.39–51.16)	37.97 ± 7.99 (18.04–50.85)	**< 0.001**	**< 0.001**	0.422
	D_{mean} (Gy)	32.06 ± 9.89 (5.89–53.11)	17.51 ± 4.49 (9.05–28.51)	18.33 ± 5.48 (8.80–33.57)	**< 0.001**	**< 0.001**	**< 0.001**
Heart	MHD (Gy)	9.07 ± 4.30 (1.27–17.46)	7.49 ± 1.77 (4.12–12.26)	7.69 ± 2.29 (4.38–14.44)	**0.004**	**0.011**	0.075
	V_{25Gy} (%)	6.21 ± 3.59 (0.01–16.28)	0.204 ± 0.399 (0–1.63)	0.715 ± 1.353 (0–7.35)	**< 0.001**	**< 0.001**	**< 0.001**

SD standard deviation, *CI* conformity index (Eq. 1), *HI* homogeneity index (Eq. 2); bold *p*-values indicate statistical significance between the three planning techniques. Range is in parentheses

(range 24.40–54.94 Gy) for 3D-CRT, 37.70 ± 7.43 (range 19.39–51.16 Gy) for IMRT and 37.97 ± 7.99 (range 18.04–50.85 Gy) for VMAT. When comparing the 3D-CRT versus IMRT plans, a reduction in D_{max} of 22.78% was observed, with a significant difference ($p < 0.001$). The D_{max} of the VMAT plans also had a significant difference ($p < 0.001$) compared to the 3D-CRT plans, with a dose reduction of 22.22%. No significant difference was observed when comparing the D_{max} between IMRT and VMAT ($p = 0.422$). The D_{mean} to the LAD-PRV was 32.06 ± 9.89 Gy (range 5.89–53.11 Gy) for 3D-CRT, 17.51 ± 4.49 (range 9.05–28.51 Gy) for IMRT and 18.33 ± 5.48 (range 8.80–33.57 Gy) for VMAT. Significant differences were present when comparing 3D-CRT with IMRT ($p < 0.001$) and VMAT ($p < 0.001$) and when comparing IMRT with VMAT ($p < 0.001$). IMRT plans presented the lowest D_{mean} among the three techniques. The D_{mean} reduction for LAD-PRV when compared to 3D-CRT was 45.38% and 42.83% for IMRT and VMAT, respectively.

The MHD of the different techniques was 9.07 ± 4.30 Gy (range 1.27–17.46 Gy) for 3D-CRT, 7.49 ± 1.77 (range 4.12–12.26 Gy) for IMRT and 7.69 ± 2.29 (range 4.38–14.44 Gy) for VMAT. A significant difference was observed when comparing 3D-CRT to IMRT ($p = 0.004$) and VMAT ($p = 0.011$). There was no significant difference between IMRT and VMAT ($p = 0.075$). The V_{25Gy} to the heart also had a decrease for modulated intensity techniques. For the 3D-CRT technique, it was 6.21 ± 3.59% (range 0.01–16.28%) while it was close to 0% for both IMRT and VMAT. The IMRT technique presented the smallest percentage of heart volume irradiated to 25 Gy. Significant differences were observed when comparing 3D-CRT to IMRT ($p < 0.001$) and VMAT ($p < 0.001$), as well as when comparing IMRT to VMAT ($p < 0.001$).

The Pearson correlation coefficients (r) between the CCD with D_{max} and D_{mean} of the LAD and the LAD-PRV are summarized in Table 2 for the three treatment techniques. In the same table, the r values for the MHD with the aforementioned doses are shown. Associations between D_{max} and D_{mean} to the LAD with their respective D_{max} and D_{mean} to the LAD-PRV are also summarized in Table 2. The p values with statistical significance are again in bold format.

Figure 3a shows the correlation between the CCD and D_{max} delivered to LAD for the three treatment techniques. According to Cohen's criteria (Cohen 1988, 1992), the three techniques presented a medium positive correlation. However, for the CCD versus D_{max} LAD relation there was no statistical significance in the VMAT plans ($p > 0.05$). The correlation for the 3D-CRT technique was the strongest among the three ($r = 0.36$, $p = 0.007$). Figure 3b shows the correlation between CCD and D_{mean} to LAD for the three techniques. All treatment modalities presented medium positive correlation according to Cohen's criteria (Cohen 1988, 1992). The 3D-CRT plans had strongest correlation ($r = 0.43$, $p < 0.001$).

The relationship of the CCD with D_{max} and D_{mean} to the LAD-PRV for the three types of plans are shown in Fig. 4a, b, respectively. All the techniques had positive correlations. However, for the CCD versus D_{max} LAD-PRV relation there was no statistical significance in the VMAT plans ($p > 0.05$). The rest of the treatment modalities had medium correlations (Cohen 1988, 1992). The strongest correlations

Table 2 Correlation between various anatomical and dosimetric parameters

Parameter	Correlation coefficient (r)		
	3D-CRT	IMRT	VMAT
CCD versus D_{max} LAD	**0.36**	**0.31**	0.30
	$p=0.007$	**$p=0.024$**	$p=0.308$
CCD versus D_{mean} LAD	**0.43**	**0.34**	**0.32**
	$p=0.001$	**$p=0.014$**	**$p=0.019$**
CCD versus D_{max} LAD-PRV	**0.33**	**0.34**	0.27
	$p=0.017$	**$p=0.013$**	$p=0.052$
CCD versus D_{mean} LAD-PRV	**0.41**	**0.36**	**0.34**
	$p=0.003$	**$p=0.009$**	**$p=0.013$**
MHD versus D_{max} LAD	0.09	**0.74**	**0.87**
	$p=0.536$	**$p<0.001$**	**$p<0.001$**
MHD versus D_{mean} LAD	**0.30**	**0.82**	**0.85**
	$p=0.028$	**$p<0.001$**	**$p<0.001$**
MHD versus D_{max} LAD-PRV	0.07	**0.60**	**0.66**
	$p=0.598$	**$p<0.001$**	**$p<0.001$**
MHD versus D_{mean} LAD-PRV	**0.31**	**0.82**	**0.87**
	$p=0.024$	**$p<0.001$**	**$p<0.001$**
D_{max} LAD versus D_{max} LAD-PRV	**0.90**	**0.92**	**0.87**
	$p<0.001$	**$p<0.001$**	**$p<0.001$**
D_{mean} LAD versus D_{mean} LAD-PRV	**0.95**	**0.99**	**0.99**
	$p<0.001$	**$p<0.001$**	**$p<0.001$**

CCD cardiac contact distance, *MHD* mean heart dose

Bold p-values indicate statistical significance

corresponded to the IMRT ($r=0.34$, $p=0.013$) and 3D-CRT ($r=0.41$, $p=0.003$) for D_{max} LAD-PRV and D_{mean} LAD-PRV, respectively.

Figure 5a–c present the relationship between the MHD and the D_{max} delivered to the LAD for the 3D-CRT, IMRT and VMAT plans, respectively. There is a drastic increase in the correlation when using modulated intensity techniques since it went from being almost non-existent for 3D-CRT and without statistical significance ($r=0.09$, $p>0.05$) to values considered large according to Cohen's criteria (Cohen 1988, 1992). The VMAT technique obtained the highest correlation value among the three ($r=0.87$, $p<0.001$).

The relationship between MHD and D_{mean} to LAD is shown in Fig. 6a–c for 3D-CRT, IMRT and VMAT techniques, respectively. The correlation coefficient increases significantly; since it goes from a medium value for 3D-CRT ($r=0.30$, $p=0.028$) to large values for both IMRT ($r=0.82$, $p<0.001$) and VMAT ($r=0.85$, $p<0.001$).

Figure 7a–c show the relationship between MHD and D_{max} LAD-PRV. The correlation increases greatly when using modulated intensity techniques, since it goes from being practically non-existent for 3D-CRT ($r=0.07$, $p=0.598$) to large values for both IMRT ($r=0.60$, $p<0.001$) and VMAT ($r=0.66$, $p<0.001$).

For the three treatment techniques, the relationship between the MHD and the D_{mean} delivered to the LAD-PRV is shown in Fig. 8. Pearson's coefficient again shows a significant increase, since it goes from a medium ($r=0.31$, $p=0.024$) to large values both in IMRT ($r=0.82$, $p<0.001$) and in VMAT ($r=0.87$, $p<0.001$).

Figure 9 shows the association between the maximum doses delivered to LAD and LAD-PRV. All techniques showed that there is a very strong correlation between D_{max} to the LAD and D_{max} to the LAD-PRV. For 3D-CRT, IMRT and VMAT plans the correlation coefficients were $r=0.90$ ($p<0.001$), $r=0.92$ ($p<0.001$) and $r=0.87$ ($p<0.001$), respectively.

Figure 10 shows the associations between the mean doses delivered to the LAD and the LAD-PRV. The correlations were very large for all three types of plans. The 3D-CRT technique had the lowest correlation ($r=0.95$, $p<0.001$)

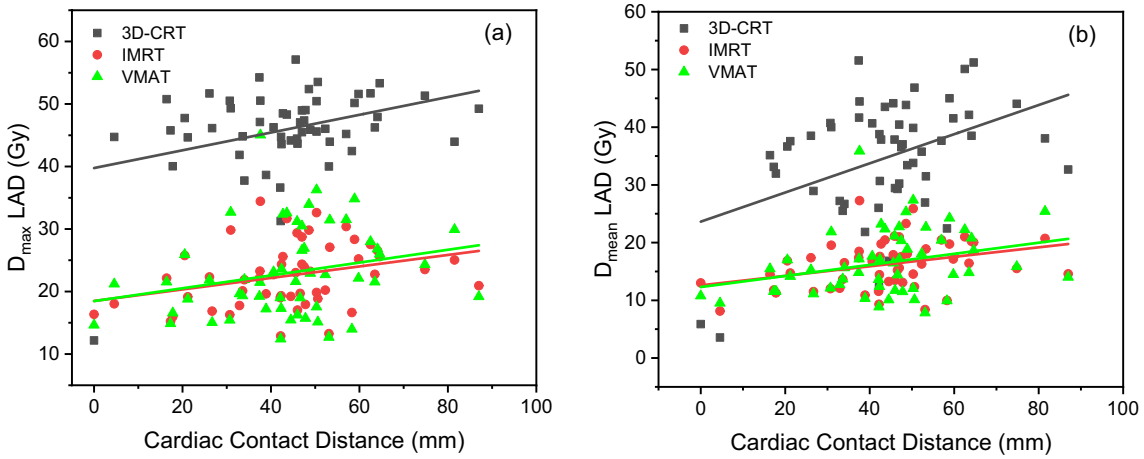

Fig. 3 Relationship between CCD and **a** D_{max} and **b** D_{mean} delivered to the LAD for the 3D-CRT, IMRT and VMAT plans

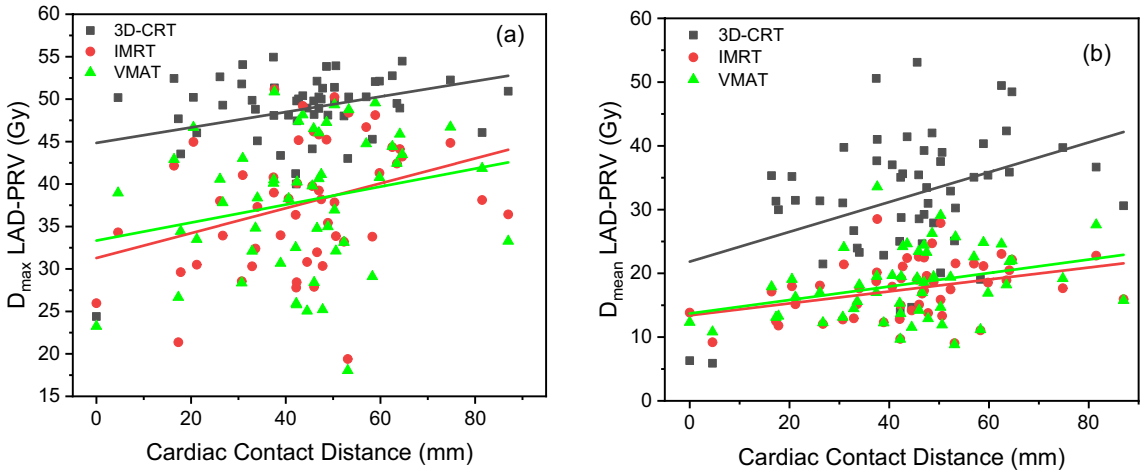

Fig. 4 Relationship between CCD and **a** D_{max} and **b** D_{mean} delivered to the LAD-PRV for the 3D-CRT, IMRT and VMAT plans

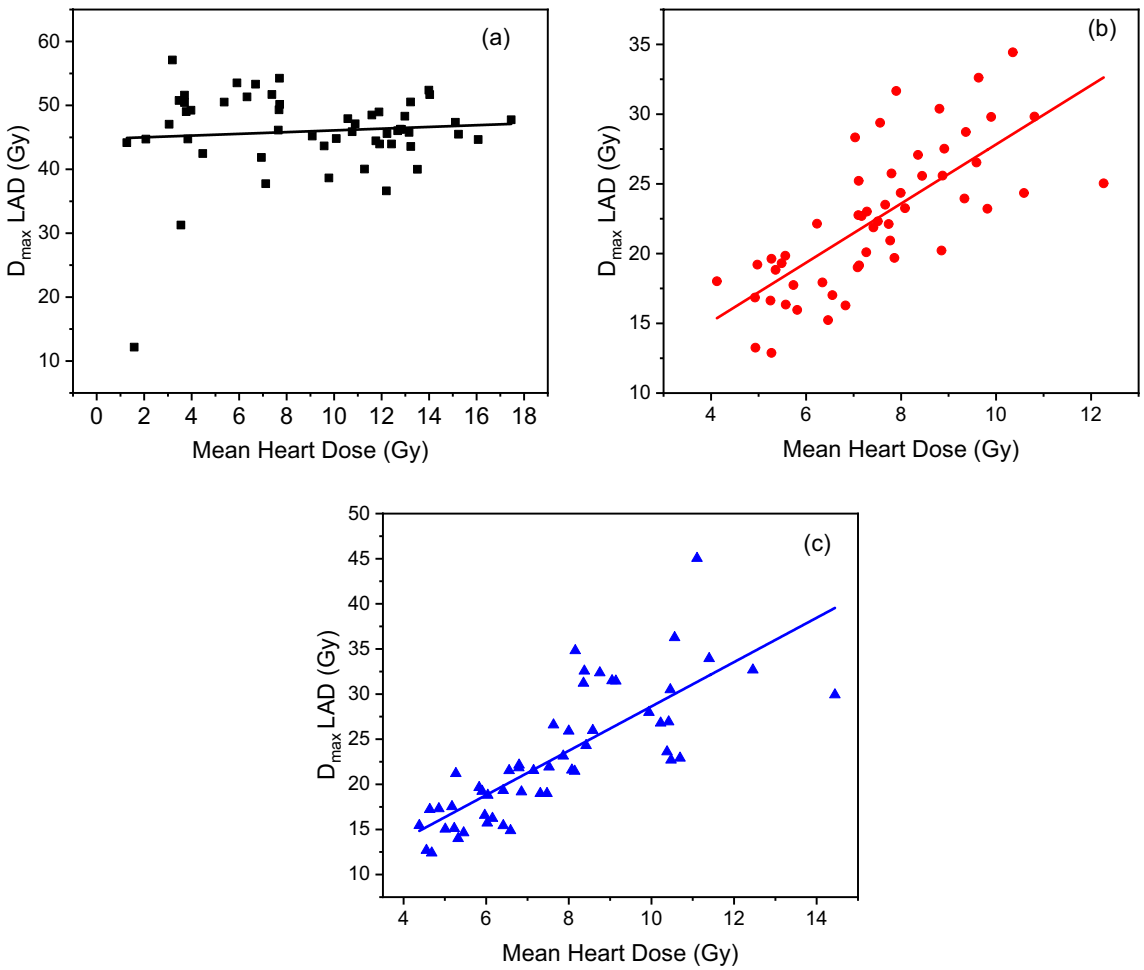

Fig. 5 Relationship between MHD and D_{max} LAD for the **a** 3D-CRT, **b** IMRT and **c** VMAT plans

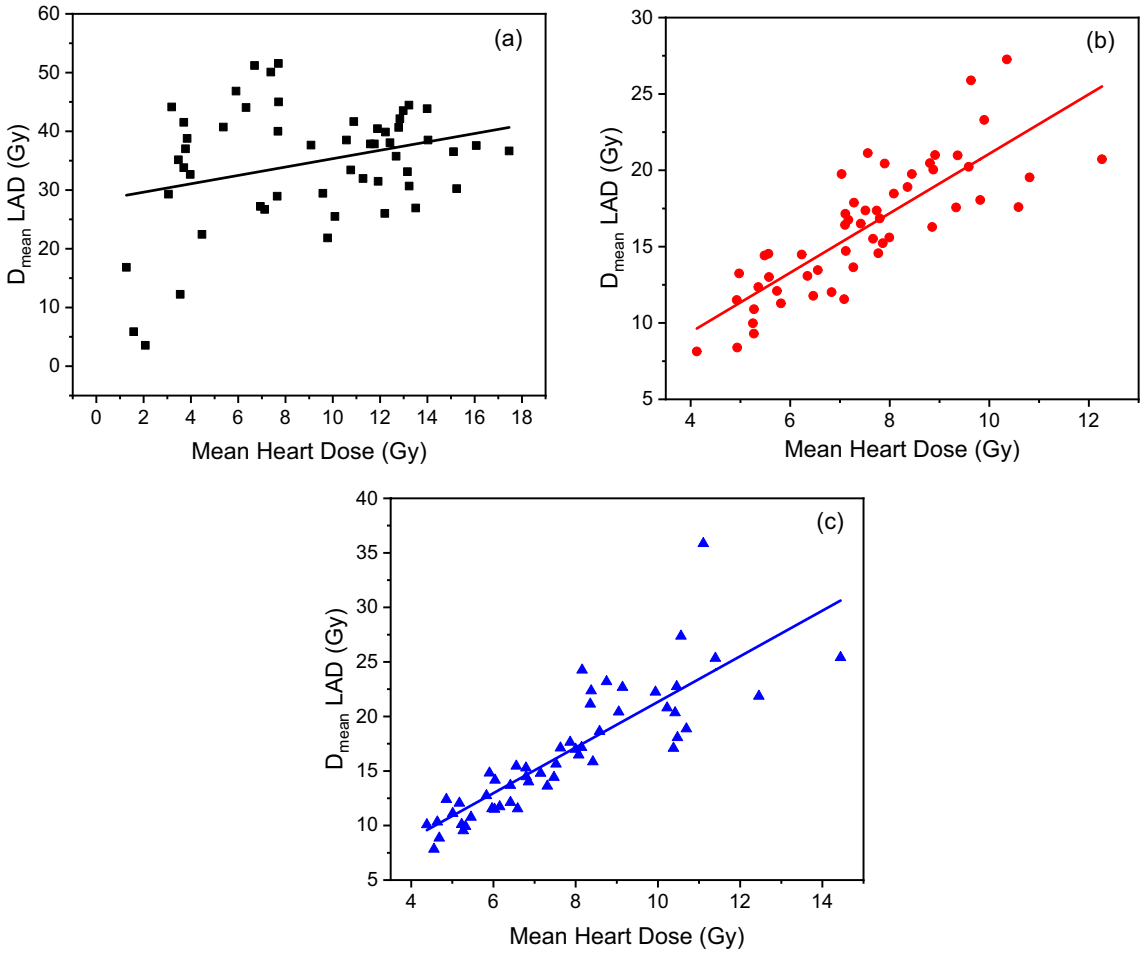

Fig. 6 Relationship between MHD and D_{mean} LAD for the **a** 3D-CRT, **b** IMRT and **c** VMAT plans

while the modulated intensity techniques had a slightly higher correlation ($r = 0.99$, $p < 0.001$).

Discussions

RT decreases the local recurrence rate and improves survival in a breast cancer scenario (Overgaard et al. 1997, 1999), however, it is also related to the presence of coronary events, particularly with the increase in the MHD (Darby et al. 2013). This information was confirmed by Van Den Bongaard et al. (2017). The adverse effects produced by RT on the breast have been studied extensively in recent years. Long-term heart damage is the main negative effect of concern. Coronary artery disease is the main cause of this (Miller et al. 2012). In the literature, it is reported that the risk of cardiac toxicity is greater for patients with left than right breast cancer (Harris et al. 2006). The introduction of modern RT techniques promises to decrease cardiac toxicity.

The sensitivity power analysis showed that a Pearson correlation coefficient with 53 participants would only be sensitive to the effects of $r = 0.33$ with a power of 80% (significance level $\alpha = 0.05$, one tail). This means that the present work would not be able to reliably detect correlations smaller than $r = 0.33$. Therefore, according to Cohen's criteria (Cohen 1988, 1992), this work would be able to adequately detect medium to large correlations. The effect size for the relationship between CCD and D_{max} to the LAD ($r = 0.36$) for the 3D-CRT plans in this work was considered to be as medium, and based on the above, it can be suggested that this study is sensitive enough to detect said effect size. In this way, the sample size of 53 patients used by the authors is more than adequate to support the idea that there is a positive correlation between CCD and the D_{max} delivered to the LAD. However, correlations lower than $r = 0.33$ were also obtained and it is therefore important to discuss the limitations of the present research. There are many ways to ensure that this work is sensitive enough to detect a given effect size, namely lowering the statistical power ($1 - \beta$) or the level of significance (α), or increasing the sample size (Lakens 2022). According to the above, a sensitivity power analysis ($\alpha = 0.05$, $1 - \beta = 0.80$, one tail) shows that for the

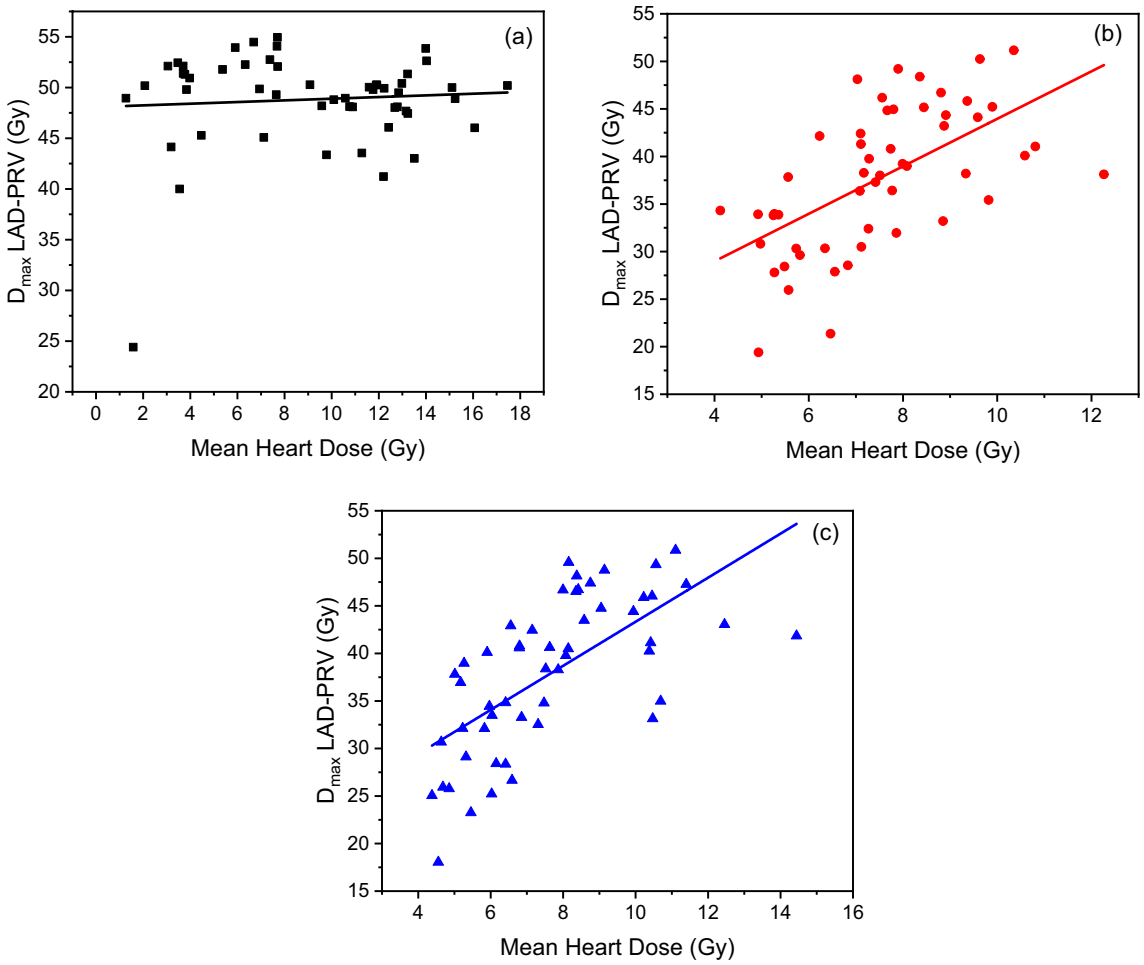

Fig. 7 Relationship between MHD and D_{max} LAD-PRV for the **a** 3D-CRT, **b** IMRT and **c** VMAT plans

present work to be sensitive enough to detect r values of 0.30, 0.20 and 0.10, it would be necessary to select 65, 147 and 564 patients, respectively. To the best of the authors' knowledge, there are very few LAD-related studies with this number of patients. Another limitation could arise if the statistical power value was increased to 90% or 95%, since this would imply that with a sample size of 53 patients ($\alpha = 0.05$, one tail) it could not be possible to correctly detect Pearson's coefficients smaller than $r = 0.38$ and $r = 0.43$, respectively. However, these power values are considered very high and are not generally used (Cohen 1988).

Previous studies have shown an association between CCD and cardiac dosimetric parameters (Wang et al. 2012; Lee et al. 2015), however, this information was focused on BCS, while not much information is available in a post-mastectomy scenario. The objective of this study was to determine the association between the CCD and the D_{max} delivered to the LAD in PMRT patients and the existence of a statistically significant positive linear correlation was demonstrated. Lee et al. (2015) reported the correlation between the mean dose to the heart and the length of the CCD. Their work employed 80 patients in a free-breathing CT, with left breast cancer and BCS. They found a correlation of $r = 0.524$. Meanwhile, Mendez et al. (2018), studied the relationship between diverse cardiac distance metrics and D_{max} and D_{mean} to the LAD. They employed 50 patients with left breast cancer and BCS. The first metric was the CCD and was defined similarly to the work of Lee et al. (2015). The other anatomical metric proposed ("4th arch") was calculated by measuring the distance from the left sternal to the beginning of the lung parenchyma edges, at the fourth costal arch level (Mendez et al. 2018). In their study, correlation coefficients $r = 0.32$ and $r = 0.49$ were found between the CCD and the MHD and D_{max} LAD, respectively. For the "4th arch" parameters, $r = 0.61$ and $r = 0.55$ were obtained for the MHD and D_{max} LAD, respectively. Based on these results, both studies suggest using these anatomical metrics as a predictor of the need to use breath-hold radiotherapy (BH) in patients with left breast cancer and BCS (Lee et al. 2015; Mendez

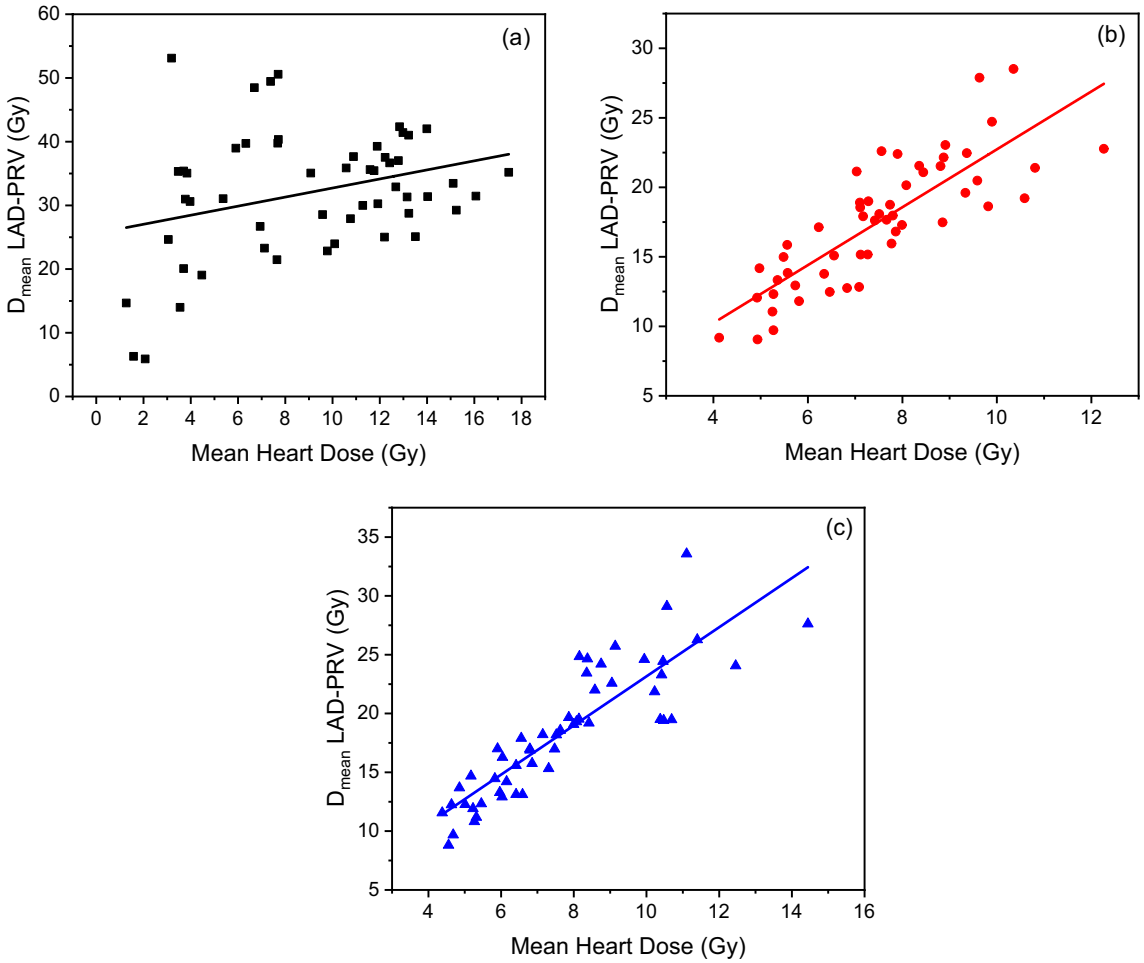

Fig. 8 Relationship between MHD and D_{mean} LAD-PRV for the **a** 3D-CRT, **b** IMRT and **c** VMAT plans

et al. 2018). Therefore, the results of this study agree with those reported in previous works.

Hiatt et al. (2006) used the CCD length measured in an axial (CCDax) and parasagittal (CCDps) planes as a tool to identify patients with "unfavorable" anatomy, which were defined as those cases where CCDax > 50 mm and CCDps > 20 mm. In a subsequent study, the same authors unsuccessfully attempted to use CCDax as a predictive tool for the irradiated volume of the heart. This was because the interaction of anatomical factors (heart, chest wall, breast) and their relationship with tangential fields was much more complex than expected (Evans et al. 2012). Based on the findings mentioned above, Rochet et al. (2015) proved that the CCDps was an adequate predictor of dose to the heart, left ventricle and LAD, that is, a higher CCDps implied a higher dose. However, in all the previous studies, only BCS patients were included. Therefore, in the present work, it has been shown that the CCD can be used as a tool to predict doses to cardiac substructures such as the LAD in PMRT.

Other studies have also tried to correlate MHD and D_{max} LAD. Aznar et al. (2011) found that although a low MHD is related to low doses of the LAD when MHD is increased it will not necessarily result in high doses of the LAD; Jacob et al. (2019) also failed to verify that MHD is an adequate predictor of dose to the coronary arteries. In the study by Atkins et al. (2021) an attempt was made to characterize these disagreements between the MHD and the LAD dose for patients with lung cancer; however, they stated that the former cannot be used to predict the dose to the latter. In this work, it was also confirmed that there is no significant association between MHD and the D_{max} LAD for plans made with tangential 3D-CRT. On the contrary, when the association between MHD and D_{mean} LAD is analyzed there is a low and statistically significant positive association ($r = 0.30$ and $p = 0.02$); this is similar to what Evans et al. (2013) reported. However, for the modulated intensity techniques there is a high correlation between the MHD and the D_{max} and D_{mean} to the LAD and LAD-PRV. This could be explained by taking into account that a fair comparison between treatment

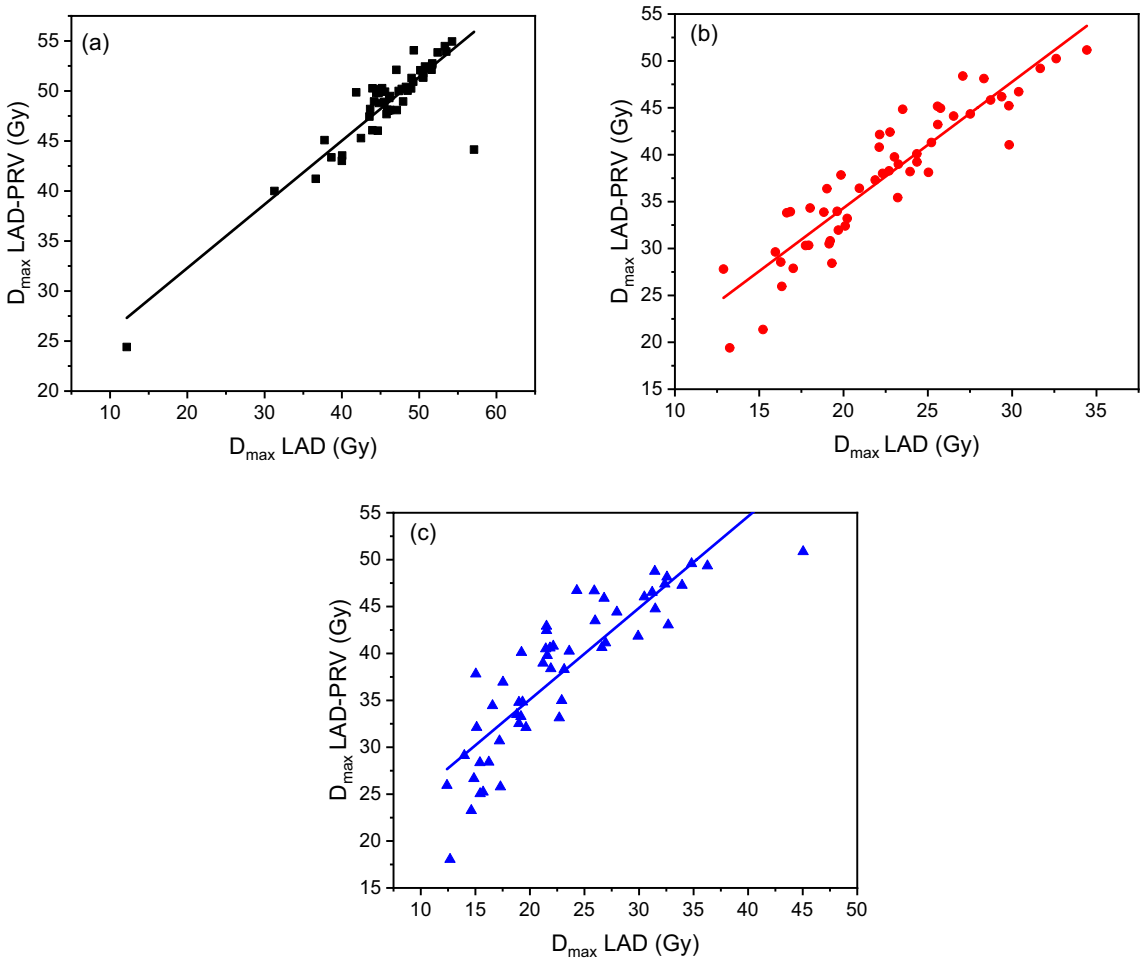

Fig. 9 Relationship between D_{max} LAD versus D_{max} LAD-PRV for the **a** 3D-CRT, **b** IMRT and **c** VMAT plans

techniques is difficult. The results depend on the choices made during the planning process, such as the constraints used and the modifications they undergo during optimization. This is particularly true for modulated intensity techniques. For certain anatomical regions, e.g. prostate, it is possible to standardize the number and angles of treatment fields for most patients. However, the anatomy of the breast is highly variable and complex, which makes it difficult to standardize the planning process in IMRT and VMAT. In this work, we sought to standardize the planning process as much as possible, using the same fields and optimization templates, but the anatomy of the patients and the target volumes were highly variable. Therefore, these differences could have influenced the dosimetric results obtained for the plans made with the modulated intensity techniques.

This study also compared free-breathing 3D-CRT, IMRT, and VMAT techniques in left-sided breast cancer patients that underwent PMRT. Modulated Intensity techniques showed better conformity and homogeneity compared to 3D-CRT. VMAT obtained the most homogeneous plans and with the best conformity (no significant difference from IMRT), while IMRT presented the lowest D_{max} and D_{mean} to LAD, and the smallest MHD and V_{25Gy} to the heart (no significant difference from VMAT). Previous studies have shown the advantages of intensity-modulated techniques compared to 3D-CRT for the entire breast in patients with early-stage breast cancer (Rudat et al. 2011; Qiu et al. 2014; Virén et al. 2015). There are reports of lower doses for various OARs such as ipsilateral lung, contralateral lung, contralateral breast, heart and LAD using IMRT or VMAT for whole breast radiotherapy (Zhou et al. 2011; Virén et al. 2015). Fiorentino et al. (2017) compared plans made with four fields of IMRT with 3D-CRT in patients with early breast cancer. Their work concluded that the IMRT plans were superior in terms of conformity, homogeneity and dose to the OARs. Hong et al. (1999) reported that the use of equally spaced angles in IMRT improves the values of CI, HI and the dose received in normal tissues. However, for post mastectomized patients with irradiation of the chest wall, information is scarce. The geometric differences

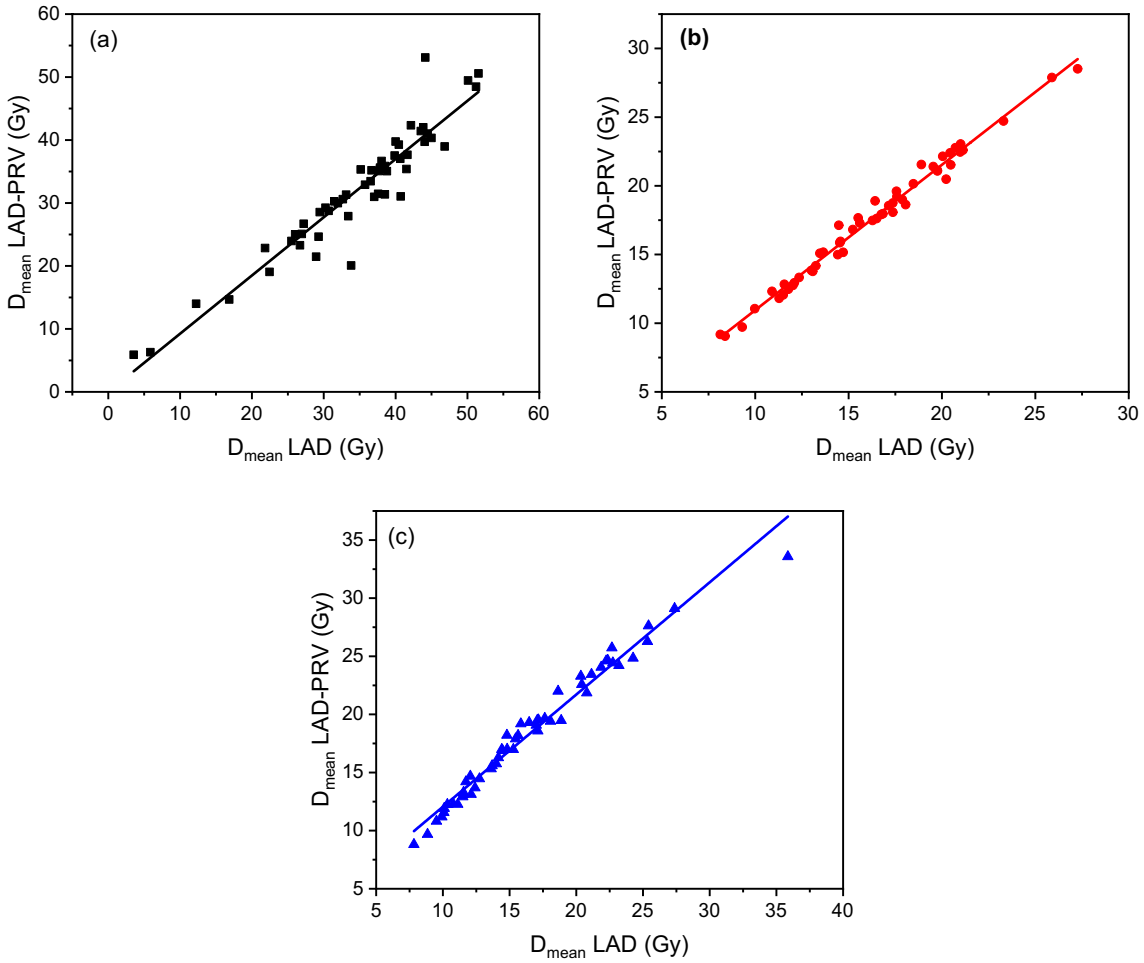

Fig. 10 Relationship between D_{mean} LAD versus D_{mean} LAD-PRV for the **a** 3D-CRT, **b** IMRT and **c** VMAT plans

between the chest wall and the whole breast are noticeable, and these differences could have an impact on the resulting dose distribution, both for the PTV and OARs (Rastogi et al. 2018). In the present work, statistically significant improvements were noted in both CI and HI when comparing 3D-CRT plans to IMRT and VMAT. Similar results were reported in the studies by Seong Hee-Khan et al. (2019) and Viköstrm et al. (2018). Additionally, the use of multiple fields of IMRT has been used to achieve high-dose sparing to the heart in early breast cancer patients with inconvenient thoracic geometry (Lohr et al. 2009; Coon et al. 2010). In the aforementioned work, IMRT was compared to 3D-CRT and a reduction in heart volumes receiving ≥ 30 Gy is reported by 87% (Lohr et al. 2009), or ≥ 35 Gy by 81% (Coon et al. 2010). These dose reductions were achieved without using techniques such as deep inspiration breath hold (DIBH) or a gating device, just as it was carried out in the present work. Furthermore, in the present study it has been shown that it is possible to reduce high doses to the LAD and to the heart by contouring the LAD, since, as previously mentioned, the plans made with 3D-CRT had not taken into account the LAD and its PRV as OARs in the planning process. As a result of contouring the LAD, the modulated intensity plans achieved a reduction of about 51% and 52% for the D_{max} and D_{mean} to the LAD, respectively. Regarding the heart, IMRT and VMAT achieved a reduction in MHD of between 15 and 17%, and for V_{25Gy} this decrease was even more dramatic, being close to 90%. This is of fundamental importance since it is recognized that $V_{25Gy} < 10\%$ is associated with a reduced probability of long-term cardiac mortality (Sardaro et al. 2012). This could be explained due to the fact that IMRT and VMAT allow a decrease in both the LAD region and the caudal part of the radiation field (Mast et al. 2013). Generally, the LAD is very close to the treatment fields, this is unavoidable due to the position of the heart and more specifically the position of the LAD in the thorax. Limiting the dose received by the caudal part of the LAD could be of great clinical relevance since Nilsson et al. (2012) described a four- to seven-fold increase in high-grade coronary stenosis after radiotherapy in the medial and distal

LAD when comparing right and left breast cancer patients. When the LAD contouring is done prospectively, the D_{max} is lower than when it's done retrospectively (Vayntraub et al. 2021); since the measurement in the present work for the 3D-CRT plans were of a retrospective nature, high doses were recorded for the LAD, therefore it is proposed that the contouring of this structure should be carried out in all left breast cancer patients who will undergo PMRT. The current trend is the transition to hypofractionated treatments (Braunstein et al. 2020), and that is why precision becomes of utmost importance. For example, Cooper et al. (2016), associated a separation of at least 2.5 mm from the LAD to the edge of a tangential field with a $D_{max} < 10$ Gy; and Wang et al. (2012), recommended to keep the LAD more than 5 mm from the edge of the tangential field.

Beaton et al. (2019) reported that the risk of cardiac death within 10 years is very low when the heart has a D_{mean} less than 3.3 Gy, and the D_{max} received by the LAD is less than 45.4 Gy. In the present study, it was possible to comply with this restriction to the D_{max} of the LAD, however, the D_{mean} to the heart was greater than 3.3 Gy for all three planning techniques. This could be explained by the fact that the planning process was done with a CT taken in free breathing. One way to achieve the aforementioned restrictions is to plan using DIBH. There is a previous study where the usefulness of sustained DIBH is recognized for the significant reduction of the dose delivered to the heart and lungs (Remouchamps et al. 2003). Quirk et al. (Quirk et al. 2020), retrospectively evaluated the dose of the LAD, in breast cancer patients who received either total breast irradiation or irradiation to the left chest wall and determined that sustained deep inspiration significantly reduces both the D_{mean} LAD and MHD. However, it was not performed in this work, since a respiratory gating device was not available in our clinic. Similarly, Poitevin-Chacón et al. (2018) obtained doses of the LAD in a range of 3.66–53.01 Gy, and for this reason they emphasize the importance of contouring the LAD and the use of DIBH to reduce cardiac doses. Other studies also suggest that doses to cardiac sub-structures should be limited in addition to the MHD. For example, Wennstig et al. (2019) suggested that limiting doses to the LAD as much as possible would reduce the risk of radiation-induced stenosis. However, many authors state that it is not possible to establish a threshold dose for the heart and LAD, this is summarized in a systematic review by Sardaro et al. (2012). Due to the above, and because the clinical effects caused by low doses of the LAD are not yet known, the authors of this work consider that the best practice is to maintain the lowest possible doses of both the heart and LAD. On the other hand, it is difficult to estimate the possible clinical effect of reducing the doses received to the heart and its substructures by the use of techniques such as IMRT and VMAT. This is because the development of radiation-related heart diseases is a very complex process since it involves many cardiac structures with different radiosensitivities (Senkus-Konefka and Jassem 2007; Darby et al. 2010). Furthermore, there are a large number of other factors that can induce the development of radiation-related heart disease, namely obesity, smoking, hypertension, use of cardiotoxic agents such as anthracyclines, taxane drugs and anti-human epidermal growth factor receptor 2 (anti-HER2) therapy. It is for all of the above that it is recommended to minimize cardiac exposure to radiation (Senkus-Konefka and Jassem 2007).

Another important factor was the thickness of the CT scan slices since it made it difficult to visualize the LAD in the distal regions. Unlike the study by Lee et al. where the tomographic slices were 2 mm (Lee et al. 2015), in this work the CT slices had a thickness of 5 mm. Anatomical atlases such as those by Feng et al. (2011) are used to correctly contour the LAD. However, the LAD is a structure with a diameter of approximately 3.7 ± 0.4 mm in the proximal parts and 1.9 ± 0.4 mm in the distal parts (Dodge et al. 1992); therefore, it is not always visible on a CT image. This causes variations in its delineation and dose evaluation (Fan et al. 2014; Kaderka et al. 2019). Lorenzen et al. (2013) even reported that there were important inter-observer disparities in LAD length that could not be reduced even using guidelines. Other factors of irregularity and uncertainty that could affect LAD contouring are cardiac and respiratory motion (White et al. 2015), CT thickness and use of intravenous contrast (Wennstig et al. 2016). Therefore, it is crucial to quantify the dosimetric impact of these uncertainties when contouring the LAD. This difficulty can be addressed by creating a structure with adequate margins around the LAD. In this way, the uncertainties described above can be covered (White et al. 2015; Wennstig et al. 2016; Duma 2017; Lee et al. 2017). White et al. (2015) used a structure with a margin of 2 mm in the anterior–posterior direction and 4 mm in the left–right plane to minimize the effects caused by cardiac and respiratory motion. For CT scans with a slice thickness of 5 mm (as it was used in the present study) Duma (2017) recommend using an auxiliary structure with a width of 5 mm in the anterior–posterior direction and 10 mm from left to right around the LAD. By adding a margin to the LAD of 6 mm Wennstig et al. (2016) were even able adequately contour the LAD using CT scans with slice thicknesses ranging from 2 to 15 mm. In other studies, the LAD was delineated without the use of contrast using anatomical references such as the anterior-interventricular groove. In addition to the above, they used a structure around the LAD made with an isotropic margin of 10 mm to limit uncertainties caused by cardiac/respiratory motion (Kirby et al. 2010). In the present study, an auxiliary structure (PRV-LAD) was used that had a diameter of 6 mm in the anterior–posterior direction and 10 mm from left to right, this agrees with the dimensions of the aforementioned studies. Additionally, in

the works of Duma (2017) and Lee et al. (2017) it is reported that there was an excellent correlation between the D_{mean} delivered to the LAD and the D_{mean} received by its auxiliary structure ($r > 0.90$). In both cases, this correlation was higher than that observed between MHD and D_{mean} LAD. This allowed them to suggest that the auxiliary structure can be used to accurately predict the dose to the LAD (Lee et al. 2017). The present work agrees with those results, that is, great correlations ($r > 0.90$) were observed for both the D_{max} and D_{mean} of the LAD with their respective D_{max} and D_{mean} for the LAD-PRV. Due to the above, it is concluded that the LAD-PRV contour ensures the adequate inclusion of the LAD. As said structure represents the relative region where the LAD is assumed to lie, it is suggested that the contouring uncertainties could be acceptable.

Based on all these studies, the present research found that the LAD and LAD-PRV are not routinely contoured in patients with postmastectomy left breast cancer. These two structures were identified as OARs and taken into account for the IMRT and VMAT planning process. This allowed to significantly reduce the doses to these structures along with the dose delivered to the heart. It is for all of the above that the authors strongly recommend the contouring of the LAD and its PRV, this becomes even more important in workplaces where it is not possible to implement techniques such as DIBH or use gating devices. This is important, since the implementation of both treatment modalities is complicated and not always possible since both require high technical, economic and human resources (Giraud and Houle 2013; Sanjoy et al. 2018).

Conclusions

In this work, it was established that CCD has a positive linear association with D_{max} to the LAD. For CT simulation protocols where it is not possible to visualize the LAD with certainty, it is possible to choose to contour an auxiliary structure around it (in this work it was the LAD-PRV) as an OAR, in this way, it is possible to ensure the adequate inclusion of the LAD, minimize uncertainties due to cardiac or respiratory motion, and improve consistency in contouring and dose reporting. There was a very high correlation between the D_{max} and D_{mean} to the LAD with their respective D_{max} and D_{mean} to the LAD-PRV, therefore the LAD-PRV could be used to accurately predict the dose to the LAD. This method could be useful for work centers where it is not possible to implement DIBH or gating devices. It was determined that modulated intensity techniques such as IMRT and VMAT made it possible to significantly reduce doses to LAD, LAD-PRV, and heart. In addition, the present work proposes that it is plausible that CCD is used as a tool to identify patients with unfavorable cardiac anatomy, where the use of 3D-CRT tangential fields would not be convenient and where the use of techniques such as IMRT and VMAT would be a better option.

Acknowledgements The authors thank the Radiotherapy Department (radiation oncologists, medical physicists, dosimetrists, radiation therapists, nurses and administrative personnel) of IMSS-UMAE Mérida for their work and invaluable collaboration.

Funding No funding.

Availability of data and material The data that support the findings of this study are available from the corresponding author E.A Martín-Tovar, upon reasonable request.

Declarations

Conflict of interest The authors declare that they have no conflict of interest.

Ethical approval All procedures performed in studies involving human participants were in accordance with the ethical standards of the institutional and/or national research committee and with the 1964 Helsinki declaration and its later amendments or comparable ethical standards.

Consent for publication Informed consent was obtained from all individual participants included in the study.

Consent to participate In this type of study formal consent is not required.

References

Atkins KM, Bitterman DS, Chaunzwa TL et al (2021) Mean heart dose is an inadequate surrogate for left anterior descending coronary artery dose and the risk of major adverse cardiac events in lung cancer radiotherapy. Int J Radiat Oncol Biol Phys. https://doi.org/10.1016/j.ijrobp.2021.03.005

Aznar M, Korreman SS, Pedersen AN et al (2011) Evaluation of dose to cardiac structures during breast irradiation. Br J Radiol 84:743–746. https://doi.org/10.1259/bjr/12497075

Beaton L, Bergman A, Nichol A et al (2019) Clinical and Translational Radiation Oncology Cardiac death after breast radiotherapy and the QUANTEC cardiac guidelines. Clin Transl Radiat Oncol 19:39–45. https://doi.org/10.1016/j.ctro.2019.08.001

Borger JH, Clinic M, Hooning MJ et al (2007) Cardiotoxic effects of tangential breast irradiation in early breast cancer patients: the role of irradiated heart volume breast cancer patients: the role of irradiated heart volume. Int J Radiat Oncol Biol Phys 69:1131–1138. https://doi.org/10.1016/j.ijrobp.2007.04.042

Bramkamp M, Rock T, Schneemann M et al (2007) Case report radiotherapy and the heart. Lancet 369:2007

Braunstein LZ, Gillespie EF, Hong L et al (2020) Breast radiation therapy under COVID-19 pandemic resource constraints d approaches to defer or shorten treatment from a comprehensive cancer center in the United States. Advancesradonc 5:582–588. https://doi.org/10.1016/j.adro.2020.03.013

Chaikh A, Giraud JY, Perrin E et al (2014) The choice of statistical methods for comparisons of dosimetric data in radiotherapy. Radiat Oncol 9:1–11. https://doi.org/10.1186/1748-717X-9-205

Cohen J (1988) Statistical power analysis for the behavioral sciences, 2nd edn

Cohen J (1992) A power primer. Psychol Bull 112:155–159. https://doi.org/10.1016/j.jorganchem.2011.01.025

Coon AB, Dickler A, Kirk MC et al (2010) Tomotherapy and multifield intensity-modulated radiotherapy planning reduce cardiac doses in left-sided breast cancer patients with unfavorable cardiac anatomy. Int J Radiat Oncol Biol Phys 78:104–110. https://doi.org/10.1016/j.ijrobp.2009.07.1705

Cooper BT, Li X, Shin SM et al (2016) Corresponding author: SC. Adv Radiat Oncol 1:373–381. https://doi.org/10.1016/j.adro.2016.08.001

Darby SC, McGale P, Taylor CW, Peto R (2005) Long-term mortality from heart disease and lung cancer after radiotherapy for early breast cancer: prospective cohort study of about 300 000 women in US SEER cancer registries. Lancet Oncol 6:557–565. https://doi.org/10.1016/S1470-2045(05)70251-5

Darby SC, Cutter DJ, Boerma M et al (2010) Radiation-related heart disease: current knowledge and future prospects. Int J Radiat Oncol Biol Phys 76:656–665. https://doi.org/10.1016/j.ijrobp.2009.09.064

Darby SC, Ewertz M, McGale P et al (2013) Risk of ischemic heart disease in women after radiotherapy for breast cancer. N Engl J Med 368:987–998. https://doi.org/10.1056/NEJMoa1209825

Dodge JT, Brown BG, Bolson EL, Dodge HT (1992) Lumen diameter of normal human coronary arteries. Influence of age, sex, anatomic variation, and Left ventricular hypertrophy or dilation. Circulation 86:232–246

Duane F, Aznar MC, Bartlett F et al (2017) Original article A cardiac contouring atlas for radiotherapy. Radiother Oncol 122:416–422. https://doi.org/10.1016/j.radonc.2017.01.008

Duma MN (2017) Tangential field radiotherapy for breast cancer—the dose to the heart and heart subvolumes: what structures must be contoured in future clinical trials? Front Oncol 7:1–6. https://doi.org/10.3389/fonc.2017.00130

Evans SB, Sioshansi S, Moran MS et al (2012) Prevalence of poor cardiac anatomy in carcinoma of the breast treated with whole-breast radiotherapy: reconciling modern cardiac dosimetry with cardiac mortality data. Am J Clin Oncol Cancer Clin Trials 35:587–592. https://doi.org/10.1097/COC.0b013e31822d9cf6

Evans SB, Panigrahi B, Northrup V et al (2013) Analysis of coronary artery dosimetry in the 3-dimensional era: implications for organ-at-risk segmentation and dose tolerances in left-sided tangential breast radiation. Pract Radiat Oncol 3:e55–e60. https://doi.org/10.1016/j.prro.2012.06.007

Fan L, Luo Y, Xu J et al (2014) A dosimetry study precisely outlining the heart substructure of left breast cancer patients using intensity-modulated radiation therapy. J Appl Clin Med Phys 15:265–274

Faul F, Erdfelder E, Lang AG, Buchner A (2007) G*Power 3: a flexible statistical power analysis program for the social, behavioral, and biomedical sciences. Behav Res Methods 39:175–191. https://doi.org/10.3758/BF03193146

Faul F, Erdfelder E, Buchner A, Lang A-G (2009) Statistical power analyses using G*Power 3.1: tests for correlation and regression analyses. Behav Res Methods 41:1149–1160. https://doi.org/10.3758/BRM.41.4.1149

Feng M, Moran J, Koelling T et al (2011) Development and validation of a heart atlas to study cardiac exposure to radiation following treatment for breast cancer. Int J Radiat Oncol Biol Phys 79:10–18. https://doi.org/10.1016/j.ijrobp.2009.10.058

Fiorentino A, Ruggieri R, Giaj-Levra N et al (2017) Three-dimensional conformal versus intensity modulated radiotherapy in breast cancer treatment: is necessary a medical reversal? Radiol Medica 122:146–153. https://doi.org/10.1007/s11547-016-0700-z

Fogliata A, Clivio A, Nicolini G et al (2007) A treatment planning study using non-coplanar static fields and coplanar arcs for whole breast radiotherapy of patients with concave geometry. Radiother Oncol 85:346–354. https://doi.org/10.1016/j.radonc.2007.10.006

Gagliardi G, Constine L, Moiseenko V et al (2010) Radiation dose–volume effects in the heart. Int J Radiat Oncol Biol Phys 76:77–85. https://doi.org/10.1016/j.ijrobp.2009.04.093

Giraud P, Houle A (2013) Respiratory gating for radiotherapy: main technical aspects and clinical benefits. Int Sch Res Not 2013:1–13. https://doi.org/10.1155/2013/519602

Harris E, Port M, Sardaro A et al (2006) Late cardiac mortality and morbidity in early-stage breast cancer patients a er breast-conservation treatment. J Clin Oncol 24:4100–4106. https://doi.org/10.1200/JCO.2005.05.1037

Hector SS, Trott KR (2007) Radiation-induced cardiovascular diseases: is the epidemiologic evidence compatible with the radiobiologic data? Int J Radiat Oncol Biol Phys 67:10–18. https://doi.org/10.1016/j.ijrobp.2006.08.071

Hiatt JR, Evans SB, Price LL et al (2006) Dose-modeling study to compare external beam techniques from protocol NSABP B-39/RTOG 0413 for patients with highly unfavorable cardiac anatomy. Int J Radiat Oncol Biol Phys 65:1368–1374. https://doi.org/10.1016/j.ijrobp.2006.03.060

Hong L, Hunt M, Chui C et al (1999) Intensity-modulated tangential beam irradiation of the intact breast. Int J Radiat Oncol Biol Phys 44:1155–1164. https://doi.org/10.1016/S0360-3016(99)00132-7

Huang B, Fang Z, Huang Y et al (2014) A dosimetric analysis of volumetric-modulated arc radiotherapy with jaw width restriction vs 7 field intensity-modulated radiotherapy for definitive treatment of cervical cancer. Br J Radiol. https://doi.org/10.1259/bjr.20140183

Jacob S, Camilleri J, Derreumaux S et al (2019) Is mean heart dose a relevant surrogate parameter of left ventricle and coronary arteries exposure during breast cancer radiotherapy: a dosimetric evaluation based on individually-determined radiation dose (BACCARA T study). Int J Radiat Oncol Biol Phys 14:1–10

Kaderka R, Gillespie EF, Mundt RC et al (2019) Geometric and dosimetric evaluation of atlas based auto-segmentation of cardiac structures in breast cancer patients. Radiother Oncol 131:215–220. https://doi.org/10.1016/j.radonc.2018.07.013

Kang S-H, Chung J-B, Kim K-H et al (2019) Comparison of dosimetrical and radiobiological parameters on three VMAT techniques for left-sided breast cancer. Prog Med Phys 30:7. https://doi.org/10.14316/pmp.2019.30.1.7

Kirby AM, Evans PM, Donovan EM et al (2010) Prone versus supine positioning for whole and partial-breast radiotherapy: a comparison of non-target tissue dosimetry. Radiother Oncol 96:178–184. https://doi.org/10.1016/j.radonc.2010.05.014

Lakens D (2022) Sample size justification collabra: psychology. Collabra Psychol 8:1–28

Lee G, Rosewall T, Fyles A et al (2015) Anatomic features of interest in women at risk of cardiac exposure from whole breast radiotherapy. Radiother Oncol 115:355–360. https://doi.org/10.1016/j.radonc.2015.05.002

Lee J, Hua K, Hsu S et al (2017) Development of delineation for the left anterior descending coronary artery region in left breast cancer radiotherapy: an optimized organ at risk. Radiother Oncol 122:423–430. https://doi.org/10.1016/j.radonc.2016.12.029

Lin JF, Yeh DC, Yeh HL et al (2015) Dosimetric comparison of hybrid volumetric-modulated arc therapy, volumetric-modulated arc therapy, and intensity-modulated radiation therapy for left-sided early breast cancer. Med Dosim 40:262–267. https://doi.org/10.1016/j.meddos.2015.05.003

Lohr F, El-Haddad M, Dobler B et al (2009) Potential effect of robust and simple IMRT approach for left-sided breast cancer on cardiac mortality. Int J Radiat Oncol Biol Phys 74:73–80. https://doi.org/10.1016/j.ijrobp.2008.07.018

Lorenzen EL, Taylor CW, Maraldo M et al (2013) Inter-observer variation in delineation of the heart and left anterior descending

coronary artery in radiotherapy for breast cancer: a multi-centre study from Denmark and the UK. Radiother Oncol 108:254–258. https://doi.org/10.1016/j.radonc.2013.06.025

Mast ME, Van Kempen-Harteveld L, Heijenbrok MW et al (2013) Left-sided breast cancer radiotherapy with and without breath-hold: does IMRT reduce the cardiac dose even further? Radiother Oncol 108:248–253. https://doi.org/10.1016/j.radonc.2013.07.017

Mège A, Ziouèche A, Pourel N, Chauvet B (2011) Toxicité cardiaque de la radiothérapie. Cancer/Radiotherapie 15:495–503. https://doi.org/10.1016/j.canrad.2011.06.003

Mendez LC, Louie AV, Moreno C et al (2018) Evaluation of a new predictor of heart and left anterior descending artery dose in patients treated with adjuvant radiotherapy to the left breast. Radiat Oncol. https://doi.org/10.1186/s13014-018-1069-z

Miller S, Zagar T, Marks LB (2012) Distribution of coronary artery stenosis after radiation for breast cancer. Breast Dis A Year B Q 23:280–282. https://doi.org/10.1016/j.breastdis.2012.06.035

Nilsson G, Holmberg L, Garmo H et al (2012) Distribution of coronary artery stenosis after radiation for breast cancer. J Clin Oncol. https://doi.org/10.1200/JCO.2011.34.5900

Overgaard M, Hansen P, Overgaard J et al (1997) Postoperative radiotherapy in high-risk premenopausal women with breast cancer who receive adjuvant chemotherapy. N Engl J Med 337:949–955

Overgaard M, Jensen M, Overgaard J et al (1999) Postoperative radiotherapy in high-risk postmenopausal breast- cancer patients given adjuvant tamoxifen: Danish Breast Cancer Cooperative Group DBCG 82c randomised trial. Lancet 353:1641–1648

Poitevin-Chacón A, Chávez-nogueda J, Prudencio RR et al (2018) Dosimetry of the left anterior descending coronary artery in left breast cancer patients treated with postoperative external radiotherapy. Reports Pract Oncol Radiother 23:91–96. https://doi.org/10.1016/j.rpor.2018.01.003

Poortmans P, Aznar M, Bartelink H (2012) Quality indicators for breast cancer: revisiting historical evidence in the context of technology changes. Semin Radiat Oncol 22:29–39. https://doi.org/10.1016/j.semradonc.2011.09.007

Popescu CC, Olivotto I, Patenaude V et al (2006) Inverse-planned, dynamic, multi-beam, intensity-modulated radiation therapy (IMRT): a promising technique when target volume is the left breast and internal mamary lymph nodes. Med Dosim 31:283–291. https://doi.org/10.1016/j.meddos.2006.05.003

Qiu JJ, Chang Z, Horton JK et al (2014) Dosimetric comparison of 3D conformal, IMRT, and V-MAT techniques for accelerated partial-breast irradiation (APBI). Med Dosim 39:152–158. https://doi.org/10.1016/j.meddos.2013.12.001

Quirk S, Grendarova P, Phan T et al (2020) A retrospective analysis to demonstrate achievable dosimetry for the left anterior descending artery in left-sided breast cancer patients treated with radiotherapy. Radiother Oncol 148:167–173. https://doi.org/10.1016/j.radonc.2020.04.022

Ramasubramanian V, Balaji K, Subramanian SB et al (2019) Hybrid volumetric modulated arc therapy for whole breast irradiation: a dosimetric comparison of different arc designs. Radiol Med 124:546–554. https://doi.org/10.1007/s11547-019-00994-1

Rastogi K, Sharma S, Gupta S et al (2018) Dosimetric comparison of IMRT versus 3DCRT for post-mastectomy chest wall irradiation. Radiat Oncol J 36:71–78. https://doi.org/10.3857/roj.2017.00381

Remouchamps V, Vicini F, Sharpe M et al (2003) Significant reductions in heart and lung doses using deep inspiration breath hold with active breathing control and intensity-modulated radiation therapy for patients treated with locoregional breast irradiation. Int J Radiat Oncol Biol Phys 55:392–406

Rochet N, Drake JI, Harrington K et al (2015) Deep inspiration breath-hold technique in left-sided breast cancer radiation therapy: Evaluating cardiac contact distance as a predictor of cardiac exposure for patient selection. Pract Radiat Oncol 5:e127–e134. https://doi.org/10.1016/j.prro.2014.08.003

Rudat V, Alaradi AA, Mohamed A et al (2011) Tangential beam IMRT versus tangential beam 3D-CRT of the chest wall in post-mastectomy breast cancer patients: a dosimetric comparison. Radiat Oncol 6:1–7. https://doi.org/10.1200/jco.2010.28.15_suppl.e11087

Sanjoy C, Santam C, Arunsingh M et al (2018) Resource requirements and reduction in cardiac mortality from deep inspiration breath hold (DIBH) radiotherapy for left sided breast cancer patients: a prospective service development analysis. Pract Radiat Oncol 8:382–387. https://doi.org/10.1016/j.prro.2018.03.007

Sardaro A, Fonte M, Patrizia M et al (2012) Radiation-induced cardiac damage in early left breast cancer patients: risk factors, biological mechanisms, radiobiology, and dosimetric constraints. Radiother Oncol 103:133–142. https://doi.org/10.1016/j.radonc.2012.02.008

Senkus-Konefka E, Jassem J (2007) Cardiovascular effects of breast cancer radiotherapy. Cancer Treat Rev 33:578–593. https://doi.org/10.1016/j.ctrv.2007.07.011

Shekel E, Levin D, Epstein D et al (2014) Is contouring the left anterior descending (lad) artery necessary for left-breast patients? A retrospective comparison between treated and revised plans. Radiat Oncol Biol 90:S265. https://doi.org/10.1016/j.ijrobp.2014.05.916

Tan W, Liu D, Xue C et al (2012) Anterior myocardial territory may replace the heart as organ at risk in intensity-modulated radiotherapy for left-sided breast cancer. Int J Radiat Oncol Biol Phys 82:1689–1697. https://doi.org/10.1016/j.ijrobp.2011.03.009

Ugurlu BT, Temelli O (2020) The impact of the field width on VMAT plan quality and the assessment of half field method. J Appl Clin Med Phys 21:115–122. https://doi.org/10.1002/acm2.12834

Van Den BVAB, Ta BDP, Van Der SA et al (2017) Validation and modification of a prediction model for acute cardiac events in patients with breast cancer treated with radiotherapy based on three-dimensional dose distributions to cardiac substructures. J Clin Oncol 35:1–8. https://doi.org/10.1200/JCO.2016.71.4113

Vayntraub A, Quinn TJ, Thompson AB et al (2021) Left anterior descending artery avoidance in patients receiving breast irradiation. Med Dosim 46:57–64. https://doi.org/10.1016/j.meddos.2020.07.006

Vikström J, Hjelstuen MH, Wasbø E et al (2018) A comparison of conventional and dynamic radiotherapy planning techniques for early-stage breast cancer utilizing deep inspiration breath-hold. Acta Oncol (Madr) 57:1325–1330. https://doi.org/10.1080/0284186X.2018.1497294

Virén T, Heikkilä J, Myllyoja K et al (2015) Tangential volumetric modulated arc therapy technique for left-sided breast cancer radiotherapy. Radiat Oncol 10:1–8. https://doi.org/10.1186/s13014-015-0392-x

Wang X, Pan T, Pinnix C et al (2012) Cardiac motion during deep-inspiration breath-hold: implications for breast cancer radiotherapy. Int Radiat Oncol Biol Phys 82:708–714. https://doi.org/10.1016/j.ijrobp.2011.01.035

Wennstig A, Garmo H, Hållström P et al (2016) Inter-observer variation in delineating the coronary arteries as organs at risk. Radiother Oncol 122:72–78. https://doi.org/10.1016/j.radonc.2016.11.007

Wennstig A, Garmo H, Isacsson U et al (2019) The relationship between radiation doses to coronary arteries and location of

coronary stenosis requiring intervention in breast cancer survivors. Radiat Oncol 14:1–11

White BM, Vennarini S, Lin L et al (2015) Accuracy of routine treatment planning 4-dimensional and deep-inspiration breath-hold computed tomography delineation of the left anterior descending artery in radiation therapy. Radiat Oncol Biol 91:825–831. https://doi.org/10.1016/j.ijrobp.2014.11.036

White J, Tai A, Arthur D et al (2018) Breast cancer atlas for radiation therapy planning: consensus definitions collaborators. Radiat Ther Oncol Group 73:1–71

Zhou GX, Xu SP, Dai X et al (2011) Clinical dosimetric study of three radiotherapy techniques for postoperative breast cancer: helical tomotherapy, IMRT, and 3D-CRT. Technol Cancer Res Treat 10:15–23. https://doi.org/10.7785/tcrt.2012.500174